Scanning-Tunneling Spectroscopy of Surface-State Electrons Scattered by a Slightly Disordered Two-Dimensional Dilute "Solid": Ce on Ag(111)

Markus Ternes,[1,*] Cédric Weber,[2] Marina Pivetta,[1] François Patthey,[1] Jonathan P. Pelz,[3] Thierry Giamarchi,[4] Frédéric Mila,[5] and Wolf-Dieter Schneider[1]

[1]*Institut de Physique des Nanostructures, École Polytechnique Fédérale de Lausanne, CH-1015 Lausanne, Switzerland*
[2]*Institut de Recherche Romand sur les Matériaux (IRRMA), EPFL, CH-1015 Lausanne, Switzerland*
[3]*Department of Physics, The Ohio State University, Columbus, Ohio 43210, USA*
[4]*DPMC, University of Geneva, Quai Enerst Ansermet 24, CH-1211 Geneva, Switzerland*
[5]*Institute of Theoretical Physics, École Polytechnique Fédérale de Lausanne, CH-1015 Lausanne, Switzerland*

(Received 16 January 2004; published 29 September 2004)

Low temperature (3.9 K) scanning-tunneling spectroscopy on a hexagonal superlattice of Ce adatoms on Ag(111) reveals site-dependent characteristic features in differential conductance spectra and in spectroscopic images at atomic-scale spatial resolution. Using a tight-binding model, we relate the overall spectral structures to the scattering of Ag(111) surface-state electrons by the Ce adatoms, the site dependence to the disorder induced by imperfections of the superlattice, and the opening of a gap in the local density of states to the observed stabilization of superlattices with adatom distances in the range of 2.3 − 3.5 nm.

DOI: 10.1103/PhysRevLett.93.146805 PACS numbers: 73.21.Cd, 68.37.Ef, 73.20.At

Two-dimensional (2D) electrons have an amazing number of remarkable properties related to correlations, magnetic field, or disorder (for a review, see, e.g., [1]). In particular, disorder is always expected to lead to Anderson localization in 2D [2], at least in the absence of correlations, with dramatic consequences on several properties, including the conductivity and the local density of states. In that context, the recent realization of a 2D hexagonal superlattice of Ce adatoms on a Ag (111) surface [3] opens new perspectives for experiment and theory: the atomic-scale spatial resolution of scanning-tunneling microscopy and spectroscopy allows direct probing of the local density of states (LDOS) of a 2D electron gas scattered by a slightly disordered periodic potential on the scale of a tenth of the lattice parameter.

In this Letter, we report the first systematic investigation of the electronic density of states of that system. The distance between two Ce adatoms in this superlattice depends on the Ce coverage, and was determined experimentally with scanning-tunneling microscopy (STM) to be in the range of $d = 2.3$ (for $\approx 1.6\%$ monolayer (ML) of Ce) to 3.5 nm (for $\approx 0.7\%$), or $\approx 8a$ to $\approx 12a$, where $a = 0.29$ nm is the nearest neighbor distance of the Ag-atoms on the Ag(111) substrate. For a given superlattice spacing d, the formation of a new 2D mini-Brillouin-zone with a concomitant splitting of the Ag(111) surface state band is expected, reminiscent of multiquantum well semiconductor heterostructures in the direction perpendicular to the multilayers [4]. Recently, such a one-dimensional step-lattice induced band-gap opening for the Shockley surface state on vicinal Cu(111) has been observed in photoemission experiments [5]. However, in contrast to this nonlocal study which averages over a macroscopic surface area, the present Ce adatom superlattice provides us with the unique opportunity to look with scanning-tunneling spectroscopy into ordered and disordered regions of a 2D solid and to map the LDOS at atomic-scale spatial resolution. We observed characteristic spectral structures and spectroscopic images which were successfully modeled within a tight-binding (TB) description of the 2D band structure, showing the opening of gaps at high-symmetry points of the superlattice Brillouin zone. In particular, the model accurately predicts the range of superlattice adatom spacings d observed for stable superlattices, as well as the influence of the adatom spacing d and local disorder on the local electronic structure.

FIG. 1 (color online). Constant current STM image (155×108 nm^2, $V_S = -90$ mV, $I = 40$ pA) of approximately 1% ML Ce with $d = 3.2$ nm on a Ag(111) surface at 3.9 K. Dark (bright) contrast: lower (upper) terrace separated by a monatomic Ag step.

The measurements were performed with a home-built STM in ultrahigh vacuum (base pressure $<10^{-8}$ Pa) at a temperature of $T = 3.9$ K by pumping on the liquid helium bath. After cleaning the Ag(111) sample by Ar-ion bombardment and annealing, Ce adatoms were deposited onto the sample at low temperature. Cut Pt-Ir wires were used as STM tips. Local spectroscopy was performed by modulating the bias voltage V_S with a sinusoidal signal ($V_{\mathrm{mod}} = 5\ \mathrm{mV_{pp}}$). All spectra were recorded by placing the tip at low tunneling current ($I = 5 - 30$ pA) and at a typical tunneling voltage of $V_S = -100$ mV above the chosen surface location and by ramping the gap voltage under open feedback-loop condition. The resulting high tunnel resistance of $R = 3 - 20$ GΩ minimizes the influence of the tip on the measurements.

Figure 1 presents a constant current STM image of the surface covered with approximately 0.01 ML Ce ($d = 3.2 \pm 0.05$ nm). Single Ce adatoms are clearly visible as bright spots forming a hexagonal superlattice. Figure 2(a) shows a STM image of a hexagonal unit cell of the Ce adatom superlattice at $T = 3.9$ K. At this temperature, the Ce adatom hopping time between neighboring Ag(111) sites is longer than the time necessary to scan the image [3]. The dI/dV spectrum shown in Fig. 2(d) was measured in the center of the triangle formed by three Ce adatoms with an adatom distance of $d = 3.2$ nm. Two relatively broad peaks are observed at approximately 85 and 210 meV. Using the energy of the first peak as the tunneling voltage for spectroscopic imaging of the differential conductance, the image of Fig. 2(b) is obtained, which shows a maximum of the LDOS in the center of the triangles, a faint one right on top of the Ce adatoms, and a minimum around the adatoms [6]. Furthermore, we found that the energy of the peaks depends strongly on the superlattice spacing d. Figure 3(a) illustrates the linear relation between the energy of the maximum of the first peak in the spectrum, measured in the center of three Ce adatoms, and the inverse area Ω^{-1} of the triangle formed by the adatoms. Figure 4 shows a slightly disordered region of Ce adatoms on Ag(111) [8]. The two spectra taken at the positions A and B show a shift of the maximum of the first peak from 85 meV (B) to 115 meV (A). The peaks are broadened in comparison with the peak in Fig. 2(d) and the intensity of the peak at around 220 meV is reduced in A and is no longer detectable in B.

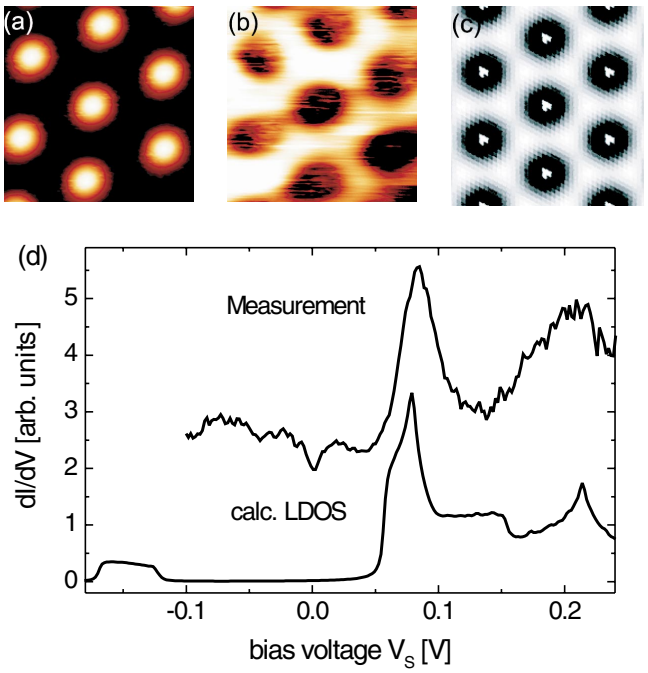

FIG. 2 (color online). (a) STM image of a hexagonal unit cell of a superlattice of Ce on Ag(111) (7.5×7.5 nm^2, $V_S = -100$ mV, $I = 10$ pA). (b) dI/dV map of the same area at the energy of the first peak (85 meV) of the spectrum shown in Fig. 2(d). (c) TB calculation of the LDOS. In white (black) the maximum (minimum) of the LDOS. (d) TB calculation and dI/dV-measurement in the center of the triangle formed by Ce adatoms (set point before opening the feedback-loop $V_S = -109$ mV, $I = 5$ pA). The calculation, in contrast to the measurement, does not include the contribution of bulk states to the LDOS.

We rationalize our experimental findings within a TB description of the surface state of Ag(111) based on the TB Hamiltonian:

$$H = -|t|\sum_{n.n.}|i\rangle\langle j| + \sum_i V_i|i\rangle\langle i| + \epsilon_0, \qquad (1)$$

where the summations run over Ag sites. We have used isotropic hopping integrals t since the surface state originates from the outer $5s^1$ electron of Ag (electronic structure $[\mathrm{Kr}]4d^{10}5s^1$), while the effect of Ce on the electronic states of Ag is described by the on-site potential V_i. As long as this potential decreases fast enough with the

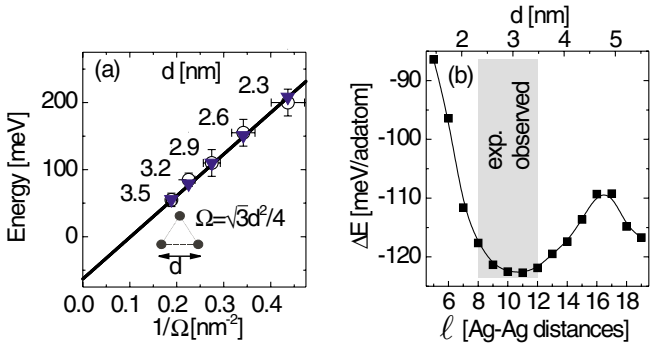

FIG. 3 (color online). (a) Energy of the maximum of the first peak in a spectrum measured in the center of three Ce adatoms as a function of the inverse area Ω^{-1} of the triangle formed by the Ce atoms (circles: measurement, triangles: TB calculation). The line is a linear fit to the measured data. (b) Energy difference ΔE between adsorbate covered and clean surface per Ce adatom calculated for each unit-cell size. The solid line is a guide for the eye.

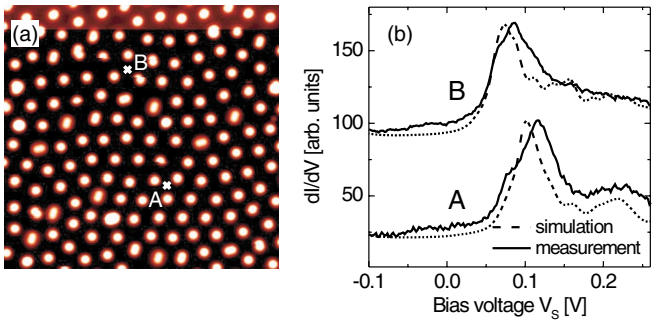

FIG. 4 (color online). (a) STM image of a slightly disordered system (35×35 nm^2, $V_S = -100$ mV, $I = 10$ pA) and (b) dI/dV spectra measured at points A and B which differ by their nearest neighbor distances. The changes in peak position, intensity, and shape in (b) indicate the sensitivity of the electronic structure to local disorder. Dashed lines: TB calculation, see text. For clarity the curves have been superimposed and curves B have been shifted vertically.

distance from the Ce atom, the results depend very little on the actual form of the potential. For simplicity, we have assumed that Ce stays in the middle of three neighboring Ag sites (hollow site) and that the effect of the Ce potential on the Ag electrons is very local: $V_i = U$ for the three Ag closest to the Ce in each unit cell, and $V_i = 0$ elsewhere [Fig. 5(b)]. The parameters $|t|$ and ϵ_0 have been

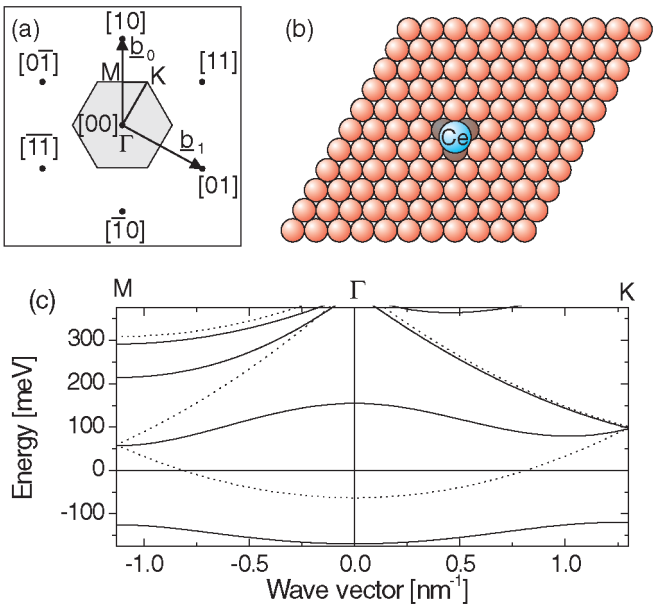

FIG. 5 (color online). (a) Characteristic points in reciprocal space. The vectors show the first two Bloch vectors. The gray area marks the 2D Brillouin zone where we find the points Γ, M, K which fulfill the Bragg condition. (b) $l \times l$ unit cell used for the TB calculation. The Ce adatom interacts only with the three nearest Ag neighbors (dark spheres). (c) Band structure of the 2D system. Dotted lines: folded dispersion of the unperturbed free electron; solid lines: TB calculation.

set to $|t| = 750$ meV and $\epsilon_0 = 4.437$ eV to reproduce the onset energy of $E_0 = -63$ meV [9] and the effective mass $m^* = 0.42 m_e$ of the surface state of Ag(111) [7], while U was adjusted to reproduce the phase shift $\delta_0 = (0.37 \pm 0.05)\pi$ deduced from the Friedel oscillations [3]. A calculation of the phase shift using our TB binding model for a single impurity (we used a 44×44 cluster with periodic boundary conditions and checked that finite-size effects were negligible) shows that this phase shift is consistent with $|U| = 1.3 \pm 0.2$ eV.

As a reference, we first calculate the band structure and the local density of states assuming a periodic arrangement of Ce adatoms. We look for the eigenstates as Bloch states of the form

$$|\psi_k\rangle = \sum_{r_i, R_m} a(r_i) e^{i\vec{k}_\parallel \cdot \vec{R}_m} |R_m, r_i\rangle, \qquad (2)$$

where R_m is the position of the unit cell containing the i^{th}Ag atom, and r_i the position of the Ag atom inside the cell, which leaves us with a $l^2 \times l^2$ (l: number of Ag atoms between two Ce adatoms) matrix to diagonalize for each wave vector. The resulting band structure is plotted in Fig. 5(c), with reciprocal basis vectors given by

$$\mathbf{b}_0 = \frac{2\pi}{d}\begin{pmatrix} 0 \\ 2/\sqrt{3} \end{pmatrix}$$

and

$$\mathbf{b}_1 = \frac{2\pi}{d}\begin{pmatrix} 1 \\ -1\sqrt{3} \end{pmatrix}$$

together with the folded band structure of the Ag(111) surface state. For a superlattice spacing of $d = 3.2$ nm, the M point is localized at $|\mathbf{k}_{\Gamma M}| = 2\pi/\sqrt{3}d = 1.13$ nm^{-1} and the K point at $|\mathbf{k}_{\Gamma K}| = 4\pi/3d = 1.31$ nm^{-1}. For an unperturbed electron gas, this corresponds to an energy of $E_M = 58$ meV and $E_K = 98$ meV. The presence of a periodic arrangement of Ce adatoms leads to the opening of gaps at the reduced-zone boundaries, and to peaks in the DOS due to the band flattening. These peaks are also reflected in LDOS, but with different amplitudes depending on the site in the unit cell. States in the lower (filled) band are concentrated close to the Ce adatoms to take advantage of the attractive potential there, while states in the upper (empty) band are concentrated at positions between the Ce adatoms. The LDOS at the center of a Ce triangle is compared to experiments in Fig. 2(d). The lowest band is between -170 and -120 meV, but its contribution to the LDOS calculated at that point is very small. Apart from the tunneling region below -100 mV, where tip-induced Ce adatom motion impedes measurement of reproducible dI/dV spectra, the agreement is remarkably good, especially considering the fact that this is not a fit but a prediction without adjusting the microscopic parameters of the model.

Using the same parameters, the shift of the energy of the first peak for different superlattices is also very well reproduced by our TB calculation [see Fig. 3(a)]. This shift varies linearly with the inverse area of the triangle formed by three adsorbates, a behavior which can also be easily understood within a model of confinement in a 2D box [10].

The TB calculation also allows us to understand why the superlattice has a "natural" periodicity of $d = 3.2$ nm. Indeed, the gap opening in the free Ag(111) band structure (which is induced by the Ce potential) increases the number of states below E_F and decreases their energy. Assuming the modified surface states are filled up to the band edge, we calculate the gain in energy, i.e., the contribution of the Ag surface-state electrons to the energy difference between Ce covered and clean surface per Ce adatom for each unit-cell size $l \times l$ [see Fig. 3(b)]. We find that the most favorable configuration corresponds to a Ce-Ce distance of 3.2 nm, precisely the distance realized experimentally in most cases. The energy gain remains significant for Ce-Ce distances in the range $d = 2.3 - 3.5$ nm, the distances found as a function of Ce adatom concentration. This effect is analogous to charge-density wave (CDW) formation in correlated systems [11], but the potential that stabilizes the CDW is external here (the Ce atoms) while it is self-consistently induced by correlations in a standard CDW. The optimal Ce-Ce distance agrees with that predicted for two adatoms by Hyldgaard and Persson [12]. They must be of the same order of magnitude since they are both related to the inverse of the Fermi wave vector of the surface-state electrons of the Ag(111) surface. However, the precise agreement suggests that the energy with several adatoms is essentially the sum of two-body interactions. Note, however, that the dramatic effects of the superlattice on the surface state (gap openings, LDOS singularities) cannot be accounted for by the model of Ref. [12].

Finally, we have studied the effect of local disorder with respect to perfect periodic arrangement of Ce adatoms on the LDOS. To compare with the experiments of Fig. 4(b), we have reproduced the local environment around points A and B inside a 44×44 cluster of Ag atoms, which was then repeated periodically to minimize finite-size effects. The agreement is again very good (see Fig. 4): the broadening and the shift of the main peaks are correctly reproduced, as well as the position of the second peak at point A and its absence at point B. Remarkably, the shifts of the main peaks agree with Fig. 3(a) if d denotes the average distance between the three Ce adatoms in the triangular lattice.

Directly over Ce adatoms, our model predicts a localized maximum in the LDOS at 85 meV (the small bright dots at the Ce atom locations in Fig. 2(c)], which is weakly discernible [Fig. 2(b)]. It also predicts an onset of the lower band near -170 meV and a band edge near -120 meV [Fig. 5(c)] which is not accessible to our experiment (see the discussion of Fig. 2(d) above). We note that the TB model does not include the atomic electron states of the Ce adatoms and the interaction between them and the Ag(111) substrate.

In conclusion, we have observed clear signatures of the effect of the Ce adatom superlattice on the surface-state electrons of Ag(111), and, with the help of a TB description of these electrons, we have proposed that the stabilization of the superlattice is a consequence of gap openings in the surface-state band. We have also shown that imperfections of the lattice lead to broadenings and shifts in the LDOS which can be reproduced by our TB description if the local geometry is taken into account. It would be interesting to go beyond this numerical approach and to investigate further the consequences of disorder. In 2D, disorder is expected to lead to Anderson localization of all states. A theoretical investigation of the local DOS in a model relevant to the present system, together with a systematic experimental mapping of the LDOS at various locations, would give access to new features of the local electronic states in 2D disordered systems.

We thank F. Silly for his early contributions to this work, R. Berndt and A. Heinrich for stimulating discussions, and the Swiss National Science Foundation for financial support.

*Electronic address: Markus.Ternes@epfl.ch

[1] G. Gat *et al.*, *Proceedings of the Conference on Physics in 2D* [Helv. Phys. Acta 65, 367 (1992)].
[2] E. Abrahams, P.W. Anderson, D.C. Licciardello, and T.V. Ramakrishnan, Phys. Rev. Lett. **42**, 673 (1979).
[3] F. Silly *et al.*, Phys. Rev. Lett. **92**, 16101 (2004).
[4] B. Tanner, *Electrons in Solids* (Cambridge University Press, Cambridge, England, 1995).
[5] F. Baumberger *et al.*, Phys. Rev. Lett. **92**, 16803 (2004).
[6] The difference between the real LDOS and dI/dV-maps at constant current due to the variation of the tip-sample distance [7] over the Ce adatoms leads to a slightly larger radius of the dark contrast region above the Ce adatoms.
[7] J. Li, W.-D. Schneider, and R. Berndt, Phys. Rev. B **56**, 7656 (1997).
[8] The disorder was estimated by applying a self correlation function to an image detail (15×15 nm^2) centered at points A and B. This analysis shows that the pattern obtained around A has a higher degree of periodicity than the one around B.
[9] M. Pivetta *et al.*, Phys. Rev. B **67**, 193402 (2003).
[10] J. Li *et al.*, Phys. Rev. Lett. **80**, 3332 (1998).
[11] *Charge Density Waves in Solids* edited by L.R. Gor'kov and G. Grüner (Elsevier, New York, 1989).
[12] P. Hyldgaard and M. Persson, J. Phys. Condens. Matter **12**, L13 (2000).